Acta Crystallographica Section A
Foundations of Crystallography
ISSN 0108-7673

Received 24 April 2007
Accepted 5 July 2007

Random tilings of compact Euclidean 3-manifolds

Juan García Escudero

Universidad Politécnica de Madrid, Departamento de Matemáticas, EUITA, Ciudad Universitaria, 28040 Madrid, Spain, and Universidad de Oviedo, Facultad de Ciencias, 33007 Oviedo, Spain. Correspondence e-mail: jjge@uniovi.es

Deterministic and random tilings for the ten compact Euclidean 3-manifolds are introduced. The main tools are substitution rules generating non-periodic planar patterns and a set of pre-axioms defined for each manifold. The sets of random tilings are obtained by suitable tile flips in the substitution atlas which allows us to compute their configurational entropies. The inflation rules in two dimensions together with one-dimensional substitutions in a perpendicular direction induce non-periodic three-dimensional tilings by triangular prisms which can be transformed into simplicial structures.

1. Introduction

Tiling models defined as projection from a lattice of higher dimension into a lower-dimension physical space have been studied in the last decades in connection with quasicrystal theory. Quasicrystal order may appear even for random tilings (Elser, 1985) and it is not yet known if deterministic tilings are better candidates than random tilings for the description of quasicrystal materials. A numerical computation of the entropy of a three-dimensional random Penrose tiling was described by Strandburg (1991). Monte Carlo simulations for rhombohedral random tiling models of icosahedral quasicrystals were performed by Shaw *et al.* (1991) and the application of transition-matrix Monte Carlo simulations by Widom *et al.* (2002) allowed them to determine the entropy of three-dimensional random rhombus tilings with high precision. In order to understand better the tiling entropy, Destainville *et al.* (2005) develop a mean field theory for random tilings based on the iterative construction of rhombus tilings introduced by de Bruijn (1981, 1986). A great deal of work has also been done on dimer models (Kenyon, 2000; Kenyon *et al.*, 2006) in connection with domino, lozenge, diabolo and other types of patterns. An extension of domino tilings of planar lattice regions to three dimensions has been considered by Randall & Yngve (2000). The tilings consist of filling octahedral and tetrahedral regions with triangular prisms. Another type of method for the generation of tilings is based on the existence of substitution or inflation rules (Escudero & Garcia, 2005). This method can be used also to generate random tilings when local rearrangements of tiles are included in the inflation rules. In this case, the configurational entropy can be computed along the lines of Escudero (2004). In contrast to the domino tilings (we do not assume here they have a vertex on the center of its long edge), which are the basis of the constructions studied by Randall & Yngve (2000), in this work we are interested in both two-dimensional and three-dimensional tilings which are always face to face.

The classification of three-dimensional crystallographic groups, achieved mainly in the 19th century, led to the determination of the ten compact Euclidean 3-manifolds (Nowacki, 1934; Hantschze & Wendt, 1935) by taking the quotient of the Euclidean space by the action of a discrete and fixed point free group of isometries (Thurston, 1997; Conway & Rossetti, 2003). Recently these spaces have been considered in cosmic crystallography. Riazuelo *et al.* (2004) investigate the signature of the 17 multiconnected flat spaces in cosmic microwave background maps. They obtain an orthonormal basis for the set of eigenvalues of the Laplace operator. Also related is the work by Rossetti & Conway (2006) where it is shown that there is, up to scale, a unique non-trivial isospectral pair of compact Euclidean 3-manifolds: only the quarter-turn space and the Hantzsche–Wendt space have identical Laplace spectra.

In recent works, non-periodic tilings for simply and multiconnected flat manifolds in two dimensions have been derived (Escudero, 2006*a*,*b*, 2007). In the present article, the results are extended to the ten compact Euclidean 3-manifolds. First, we consider finite triangle patterns which form the pre-axioms for two of the fundamental polyhedra faces. These have been chosen in order to have face-to-face patterns after the corresponding identifications. With the help of two-dimensional substitutions applied to the two triangular faces of the basic prisms and the Cartesian product of two one-dimensional substitutions for the three rectangular faces, we obtain the desired three-dimensional structures, which can later be decomposed in order to get simplicial tilings. The two basic planar patterns have 8-fold and 12-fold symmetries. The octagonal pattern was generated by Escudero (2000) by extending the construction of Nischke & Danzer (1996) to even symmetries. The dodecagonal pattern can be derived with the help of the constructions studied by Escudero (2001,

2003). Both patterns are deterministic and we introduce random tilings which are defined by means of local rearrangements of tiles appearing in the inflation rules. In three dimensions, they are induced by the two-dimensional random substitutions, and the configurational entropy depends only on tile rearrangements in the faces of the fundamental polyhedra.

2. Deterministic tilings for Euclidean 2-manifolds

In this section, we first introduce two substitution tilings of the Euclidean plane $\mathcal{T}il_d$, $d = 8, 12$, and then we show how the same sets of inflation rules can be used in order to generate tilings of the flat torus and the Klein bottle. The two-dimensional tilings are described in terms of word sequences in D0L systems.

Definition 1. A 0L system is a triple $G = \{\Sigma, h, \omega\}$, where $\Sigma = \{x_1, x_2, \ldots, x_n\}$ is an alphabet, h is a finite substitution on Σ into the set of subsets of Σ^* and $\omega \in \Sigma^*$ is the axiom. G is called a D0L system if $\#(h(x_i)) = 1$, for every x_i in Σ.

The first type of structures $\mathcal{T}il_8$ were studied by Escudero (2006*b*) for the generation of tilings for two-dimensional flat manifolds. The letters a_m, b_m, c_m, d_m, e_m represent the prototiles

$$\mathcal{T}(B, A, C), \quad \mathcal{T}(C, B, C), \quad \mathcal{T}(A, A, B), \quad \mathcal{T}(B, B, D), \quad \mathcal{T}(C, A, D), \tag{1}$$

respectively, where A, B, C, D have lengths s_1, s_2, s_3, s_4, with $s_k \equiv \sin(k\pi/8)$. $\mathcal{T}(X, Y, Z)$ is a triangular tile with edges X, Y, Z placed anticlockwise and the index $m \in Z_{16}$ denotes relative orientation. The tile $\mathcal{T}(X, Y, Z)$ with the edge Z placed on the positive x axis corresponds to the index 1. The oriented tile with index m is obtained by a rotation of $\pi(m-1)/8$ through the left-most vertex. The alphabet is

$$\Sigma = \{a_m, \widetilde{a}_m, b_m, c_m, d_m, e_m, \widetilde{e}_m, (,)\} \tag{2}$$

with $m \in Z_{16}$. It contains two brackets and letters of type t_i and $\widetilde{t}_i$. The tile $\widetilde{t}_1$ is obtained by a reflection of t_1 in a line perpendicular to the edge Z. The set of production rules h is (Fig. 1*a*)

$$\begin{aligned}
a_m &\longmapsto (\Phi_8[a_m]) = (\widetilde{a}_{m+7}\widetilde{e}_m\widetilde{b}_{m+1}d_{m+10}) \\
b_m &\longmapsto (\Phi_8[b_m]) = (\Phi_8[a_m]\Phi_8[c_{m-5}]\Phi_8[\widetilde{a}_{m+6}]) \\
c_m &\longmapsto (\Phi_8[c_m]) = (\widetilde{e}_{m+7}e_{m+9}) \\
d_m &\longmapsto (\Phi_8[d_m]) = ((a_{m+6}d_{m-1}\Phi_8[c_m])(\widetilde{a}_{m+10}d_{m+1}b_{m+4}b_{m+6})) \\
e_m &\longmapsto (\Phi_8[e_m]) = (c_{m+7}\widetilde{a}_m d_{m+7}b_{m+10}b_{m+12}\widetilde{e}_{m+11}) \\
) &\longmapsto) \\
(&\longmapsto (.
\end{aligned} \tag{3}$$

Throughout this paper, the term axiom is used to indicate both a word and a geometric pattern. By iterating the production rules applied to any letter representing a tile, we get word sequences describing the tiling growth. The geometric interpretation of the word sequences is as follows. In the word $(\widetilde{a}_{m+7}\widetilde{e}_m\widetilde{b}_{m+1}d_{m+10})$, if two letters follow one another inside a bracket, the corresponding oriented triangles are glued face to face in a unique way. In the next derivation step, which gives $((\Phi_8[\widetilde{a}_{m+7}])(\Phi_8[\widetilde{e}_m])(\Phi_8[\widetilde{b}_{m+1}])(\Phi_8[d_{m+10}]))$, two oriented triangles represented by consecutive words enclosed by brackets like $\Phi_8[\widetilde{a}_{m+7}]$ and $\Phi_8[\widetilde{e}_m]$ are glued face to face and again the prescription is unique. For the edge word sequences, the alphabet is $\Sigma = \{A, B, C, D\}$, and the production rules are

$$\begin{aligned}
A &\longmapsto \phi_8[A] = D \qquad B \longmapsto \phi_8[B] = CC \\
C &\longmapsto \phi_8[C] = BDB \quad D \longmapsto \phi_8[D] = ACCA.
\end{aligned} \tag{4}$$

Now we consider the tiling $\mathcal{T}il_{12}$. The triangle edges, denoted by A, B, C, D, E, F, have lengths $s_1, s_2, s_3, s_4, s_5, s_6$, where $s_k \equiv \sin(k\pi/12)$. The letters $\alpha_m, \beta_m, \gamma_m, \delta_m, \epsilon_m, \zeta_m, \eta_m, \theta_m, \lambda_m, \mu_m, \nu_m, \xi_m$ represent the prototiles

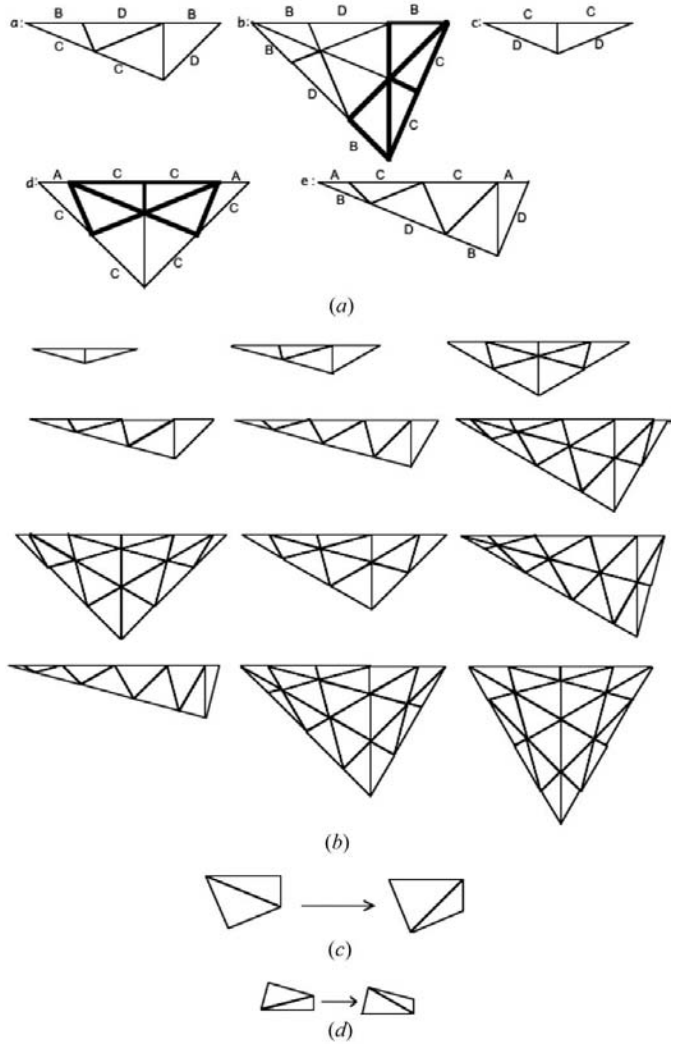

Figure 1
(*a*) Inflation rules for $d = 8$ with potential regions for flips marked, (*b*) inflation rules for $d = 12$, and tile rearrangements in the inflation rules for (*c*) $d = 8$: $d_{m-1}\widetilde{e}_{m+7} \Rightarrow b_{m+10}a_{m+2}$, (*d*) $d = 12$: $\zeta_{m+13}\mu_{m+1} \Rightarrow \lambda_{m+12}\widetilde{\epsilon}_{m+10}$.

$$\mathcal{T}(A,A,B),\mathcal{T}(B,A,C),\mathcal{T}(B,B,D),\mathcal{T}(C,A,D),\mathcal{T}(D,A,E),\mathcal{T}(D,B,F),\mathcal{T}(C,C,F),\mathcal{T}(C,B,E),\mathcal{T}(E,B,E),\mathcal{T}(E,A,F),\mathcal{T}(D,C,E),\mathcal{T}(D,D,D). \quad (5)$$

The alphabet is

$$\Sigma = \{\alpha_m, \beta_m, \widetilde{\beta}_m, \gamma_m, \delta_m, \widetilde{\delta}_m, \epsilon_m, \widetilde{\epsilon}_m, \zeta_m, \widetilde{\zeta}_m, \eta_m, \theta_m, \widetilde{\theta}_m, \lambda_m, \widetilde{\lambda}_m, \mu_m, \widetilde{\mu}_m, \nu_m, \widetilde{\nu}_m, \xi_m, (,)\} \quad (6)$$

with $m \in Z_{24}$. The production rules h in this case are (Fig. 1*b*)

$$\begin{aligned}
\alpha_m &\longmapsto (\Phi_{12}[\alpha_m]) = (\widetilde{\mu}_{m+11}\mu_{m+13})\\
\beta_m &\longmapsto (\Phi_{12}[\beta_m]) = (\widetilde{\epsilon}_{m+11}\widetilde{\mu}_m\lambda_{m+1}\zeta_{m+14})\\
\gamma_m &\longmapsto (\Phi_{12}[\gamma_m]) = ((\widetilde{\theta}_{m+10}\widetilde{\xi}_{m-1}\widetilde{\nu}_{m+10}\nu_{m+14})\\
&\qquad (\widetilde{\mu}_{m+11}\mu_{m+13}\zeta_{m+1}\theta_{m+14}))\\
\delta_m &\longmapsto (\Phi_{12}[\delta_m]) = (\widetilde{\delta}_{m+11}\widetilde{\epsilon}_m\widetilde{\xi}_{m+11}\lambda_{m+14}\widetilde{\nu}_{m+2}\eta_{m+15})\\
\epsilon_m &\longmapsto (\Phi_{12}[\epsilon_m]) = (\widetilde{\beta}_{m+11}\widetilde{\delta}_m\widetilde{\theta}_{m+11}\widetilde{\xi}_m\widetilde{\nu}_{m+11}\nu_{m+15}\widetilde{\nu}_{m+3}\widetilde{\zeta}_{m+16})\\
\zeta_m &\longmapsto (\Phi_{12}[\zeta_m]) = ((\beta_{m+10}\gamma_{m-1}\theta_{m+10}\eta_{m-1}\nu_{m+10}\xi_{m+7}\nu_{m+18}\lambda_{m+6})\\
&\qquad (\Phi_{12}[\gamma_m]\widetilde{\zeta}_{m+3}\widetilde{\epsilon}_{m+16}))\\
\eta_m &\longmapsto (\Phi_{12}[\eta_m]) = ((\delta_{m+9}\theta_{m-2}\widetilde{\theta}_{m+10}\widetilde{\zeta}_{m-1}\widetilde{\mu}_{m+11}\mu_{m+13})\\
&\qquad (\zeta_{m+9}\nu_{m-2}\widetilde{\nu}_{m+18}\nu_{m+14}\zeta_{m+1}\theta_{m+14})\\
&\qquad (\widetilde{\nu}_{m+18}\nu_{m+6}\widetilde{\nu}_{m+2}\zeta_{m+15}\widetilde{\theta}_{m+2}\widetilde{\delta}_{m+15}))\\
\theta_m &\longmapsto (\Phi_{12}[\theta_m]) = ((\gamma_{m+10}\widetilde{\theta}_{m-1}\eta_{m+10}\widetilde{\nu}_{m-1}\xi_{m+2}\widetilde{\nu}_{m+15})\\
&\qquad (\widetilde{\epsilon}_{m+11}\widetilde{\mu}_m\lambda_{m+1}\zeta_{m+14}\eta_{m+2}\widetilde{\theta}_{m+15}))\\
\lambda_m &\longmapsto (\Phi_{12}[\lambda_m]) = ((\Phi_{12}[\epsilon_m]\widetilde{\mu}_{m+4})\\
&\qquad (\beta_{m-1}\delta_{m+10}\theta_{m-1}\zeta_{m+10}\nu_{m-1}\widetilde{\nu}_{m+19}\nu_{m+7}\\
&\qquad \zeta_{m+18}\mu_{m+6}))\\
\mu_m &\longmapsto (\Phi_{12}[\mu_m]) = (\alpha_{m+11}\widetilde{\beta}_m\gamma_{m+11}\widetilde{\theta}_m\eta_{m+11}\widetilde{\nu}_m\xi_{m+3}\widetilde{\nu}_{m+16}\mu_{m+18}\\
&\qquad \widetilde{\mu}_{m+17})\\
\nu_m &\longmapsto (\Phi_{12}[\nu_m]) = ((\widetilde{\epsilon}_{m+11}\widetilde{\mu}_m\lambda_{m+1}\zeta_{m+14}\eta_{m+2}\widetilde{\theta}_{m+15}\widetilde{\epsilon}_{m+3})\\
&\qquad (\gamma_{m+10}\widetilde{\theta}_{m-1}\eta_{m+10}\widetilde{\nu}_{m-1}\xi_{m+2}\widetilde{\nu}_{m+15}\lambda_{m+17}\widetilde{\mu}_{m+16})\\
&\qquad (\delta_{m-2}\epsilon_{m+9}\zeta_{m-2}\lambda_{m+9}\widetilde{\nu}_{m+7}\eta_{m+18}\zeta_{m+6}))\\
\xi_m &\longmapsto (\Phi_{12}[\xi_m]) = ((\widetilde{\theta}_{m+10}\theta_{m-2}\zeta_{m+9}\nu_{m-3}\widetilde{\nu}_{m+19})\\
&\qquad (\widetilde{\mu}_{m+11}\widetilde{\zeta}_{m-1}\widetilde{\nu}_{m+10}\nu_{m-2}\widetilde{\nu}_{m+18}\widetilde{\xi}_{m+7}\widetilde{\theta}_{m+18})\\
&\qquad (\mu_{m+13}\zeta_{m+1}\nu_{m+14}\widetilde{\nu}_{m+2}\nu_{m+6}\zeta_{m+17}\theta_{m+6})\\
&\qquad (\theta_{m+14}\widetilde{\theta}_{m+2}\widetilde{\zeta}_{m+15}\widetilde{\nu}_{m+3}\nu_{m+5}))\\
)&\longmapsto)\\
(&\longmapsto (\qquad (7)
\end{aligned}$$

and the edge substitution rules are

$$\begin{aligned}
A &\longmapsto \phi_{12}[A] = F & B &\longmapsto \phi_{12}[B] = EE\\
C &\longmapsto \phi_{12}[C] = DFD & D &\longmapsto \phi_{12}[D] = CEEC \quad (8)\\
E &\longmapsto \phi_{12}[E] = BDFDB & F &\longmapsto \phi_{12}[F] = ACEECA.
\end{aligned}$$

The inflation rules given by equations (3) and (7) can be used for the construction of substitution tilings for the Euclidean torus T^2 and the Euclidean Klein bottle K^2 [see Fig. 2(*a*) for the principle of gluing on their fundamental polygons]. We can use the same previously defined D0L systems except the axiom $\omega = \Phi_d[\Xi]$, where Ξ denotes the pre-axiom.

A pre-axiom for T^2 and K^2 tilings is [see Fig. 2(*b*) left and the pattern in Fig. 3]

$$\Xi = \widetilde{e}_{10}e_{12}\widetilde{e}_2e_4d_{12}b_{15}b_1d_{10}a_1\widetilde{a}_{13}d_4b_7b_9d_2a_9\widetilde{a}_5. \quad (9)$$

For a K^2 tiling, we can choose (Fig. 2*b*, right)

$$\Xi = d_9b_{12}b_{14}a_6e_{13}a_{12}e_3e_{11}a_4\widetilde{a}_{12}\widetilde{e}_5b_6b_4d_1. \quad (10)$$

Other axioms are possible (Fig. 2*c*), also based on the tiles given by equation (5) (see for instance the pre-axiom for the hexagonal face of $c1$ in Fig. 6 which is valid also for the

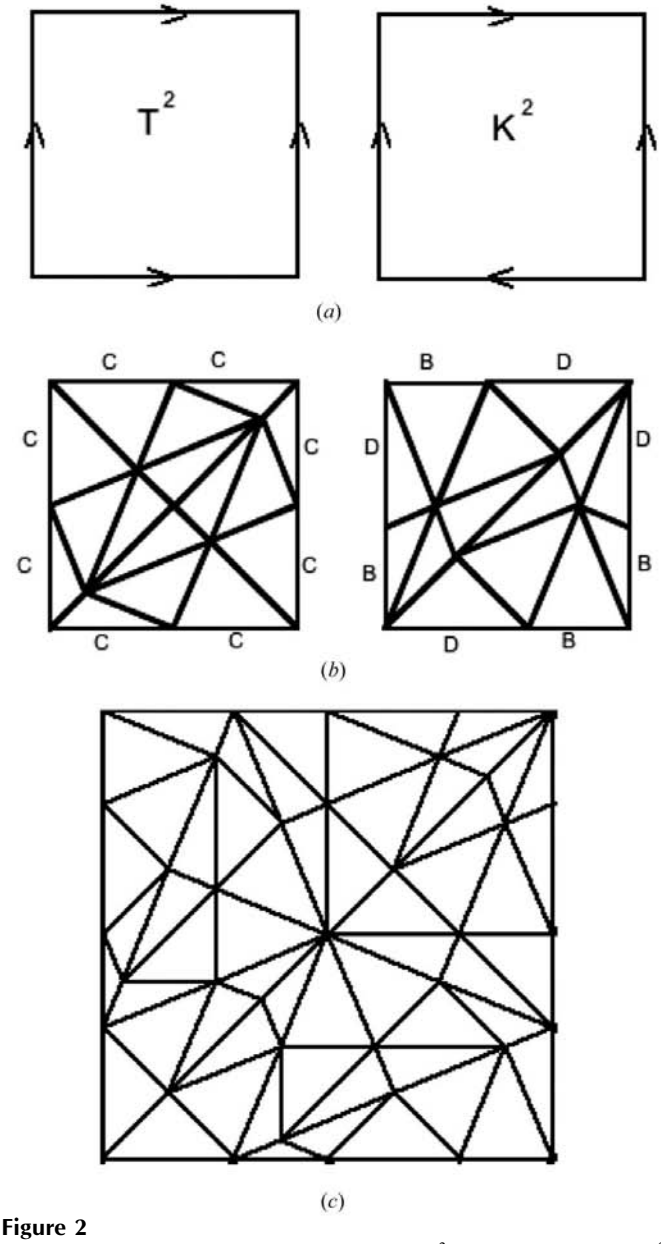

Figure 2
(*a*) Principle of gluing for the Euclidean torus T^2 and the Klein bottle K^2. (*b*) Pre-axioms for T^2 and K^2 (left) and for K^2 (right). (*c*) Pre-axiom for T^2.

hexagonal T^2). Once we give the substitution atlas and the pre-axioms, which represent face-to-face patterns, the fact that the tilings will be always face to face in the derivation process is a consequence of the form of equations (4) and (8) defining the edge inflation rules. The reason is that, for any edge X, both satisfy

$$\phi_d(X) = \mathrm{Mir}(\phi_d(X)), \tag{11}$$

where the mirror image of a word w is represented by $\mathrm{Mir}(w)$. The resulting words are palindromes and therefore the tilings satisfy the face-to-face condition.

3. Configurational entropy for non-deterministic patterns

The tilings discussed in the previous section are deterministic, in the sense that only one production rule is allowed for each letter at every step in the derivation process. We introduce random tilings by means of local rearrangements of tiles in the substitution rules. For $d = 8$, an edge flip induces the following tile rearrangement (see Fig. 1*c*):

$$d_{m-1}\widetilde{e}_{m+7} \Rightarrow b_{m+10}a_{m+2} \tag{12}$$

and for $d = 12$ (Fig. 1*d*)

$$\zeta_{m+13}\mu_{m+1} \Rightarrow \lambda_{m+12}\widetilde{\epsilon}_{m+10}. \tag{13}$$

Definition 2. The configurational entropy per tile S is the logarithm of the number of tilings of a given size and shape divided by the number of tiles, in the thermodynamic limit.

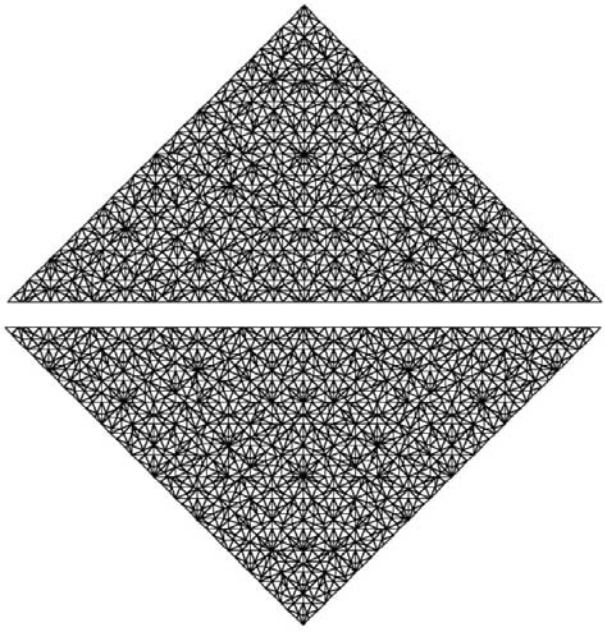

Figure 3
Applying four times the inflation rules given by equation (3) to d_1 and d_9 and gluing through the edge D, we get the fundamental polygon. This derivation corresponds to the pre-axiom of Fig. 1(*b*), which is valid for both T^2 and K^2.

For the derivation of the entropy, we identify congruent prototiles and we take into account only the tile contents in the first inflation step given by equations (3) and (7) and not the tile orientations. The frequency of the tile x is denoted by $\mathcal{F}_x$.

Proposition 1. The configurational entropy for the tilings defined by equation (3) and tile rearrangements given by equation (12) is

$$S = \frac{2}{3+2\sqrt{2}}(\mathcal{F}_b + \mathcal{F}_d)\,\mathrm{Log}\,2 \approx 0.145. \tag{14}$$

Proof: The frequencies of the tiles $\mathcal{F}_a, \mathcal{F}_b, \mathcal{F}_c, \mathcal{F}_d, \mathcal{F}_e$ in the tiling are given by the elements of the normalized eigenvector corresponding to the eigenvalue with largest modulus of the substitution matrix. The normalized eigenvector associated with the eigenvalue $\sigma = 4 + 2\sqrt{2}$, highest root of $x^2 - 8x + 8$, is

$$\left(\frac{31+22\sqrt{2}}{a}, \frac{1}{3}, \frac{13+9\sqrt{2}}{a}, \frac{62+44\sqrt{2}}{a}, \frac{44+31\sqrt{2}}{a}\right) = (\mathcal{F}_a, \mathcal{F}_b, \mathcal{F}_c, \mathcal{F}_d, \mathcal{F}_e), \tag{15}$$

where $a = 225 + 159\sqrt{2}$. The general solution to the difference equation

$$T(n+3) = 6T(n+2) + 8T(n+1) - 16T(n) \tag{16}$$

is

$$T(n) = k_1(-2)^n + k_2 8^n \sigma^{-n} + k_3 \sigma^n. \tag{17}$$

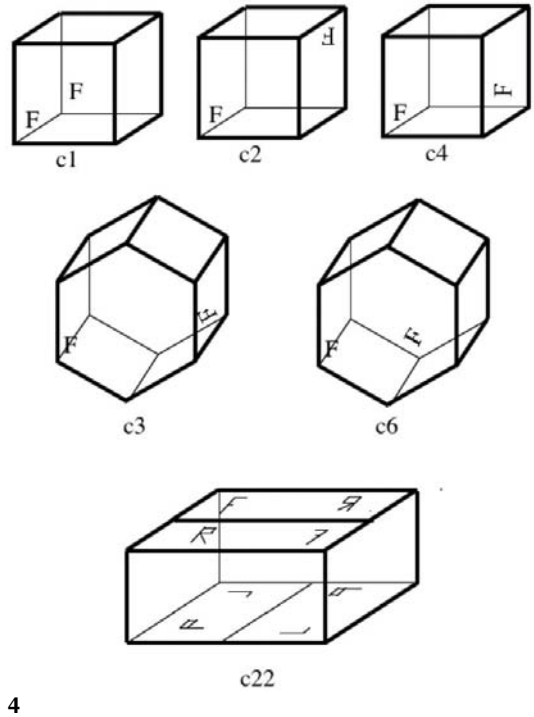

Figure 4
Fundamental domains for the compact orientable flat manifolds.

The number of b and d tiles after n iterations is $N_n^b = k_1^b(-2)^n + k_2^b 8^n \sigma^{-n} + k_3^b \sigma^n$ and $N_n^d = k_1^d(-2)^n + k_2^d 8^n \sigma^{-n} + k_3^d \sigma^n$, respectively, and the total number of tiles is $N_n = k_1(-2)^n + k_2 8^n \sigma^{-n} + k_3 \sigma^n$, where k_i^b, k_i^d, k_i are constants determined by the initial conditions of the tiles' content.

We find two copies of $d_{m-1}\widetilde{e}_{m+7}$ in $\Phi_8[b_n]$ and two in $\Phi_8[d_n]$ (see Fig. 1*a*). By taking into account

$$\lim \frac{N_m^b}{N_m} = \frac{k_3^b}{k_3}, \quad \lim \frac{N_m^d}{N_m} = \frac{k_3^d}{k_3}, \tag{18}$$

and that the number of patterns after iterating n times is

$$2^{2\sum_{m=1}^{n-1}(N_m^b + N_m^d)}, \tag{19}$$

we conclude that equation (14) is satisfied. □

The corresponding result for $d = 12$ is given by

Proposition 2. The configurational entropy for the tilings defined by equation (7) and tile rearrangements given by equation (13) is

$$S = \frac{1}{7 + 4\sqrt{3}}[2(\mathcal{F}_\gamma + \mathcal{F}_\eta + \mathcal{F}_\lambda) + 6\mathcal{F}_\xi]\,\mathrm{Log}\,2 \approx 0.073. \tag{20}$$

Proof: In this case, we consider the difference equation

$$\begin{aligned} T(n+8) = {} & 9T(n+7) + 114T(n+6) - 296T(n+5) \\ & - 1440T(n+4) + 2448T(n+3) + 2720T(n+2) \\ & - 2304T(n+1) - 1536T(n) \end{aligned} \tag{21}$$

with general solution

$$\begin{aligned} T(n) = {} & k_1(-1)^n + k_2(2)^n + k_3(-2\sqrt{3})^n + k_4(2\sqrt{3})^n \\ & + k_5(-2 - 2\sqrt{3})^n + k_6 4^n(2 - 2\sqrt{3})^n + k_7 2^n(-2 + \sqrt{3})^n \\ & + k_8 4^n(2 + \sqrt{3})^n. \end{aligned} \tag{22}$$

Now we have two copies of $\zeta_{m+13}\mu_{m+1}$ in $\Phi_{12}[\gamma_n]$, $\Phi_{12}[\eta_n]$, $\Phi_{12}[\lambda_n]$ and six in $\Phi_{12}[\xi_n]$. By using *Mathematica* (Wolfram, 1991), we get

$$\mathcal{F}_\gamma \approx 0.0548, \ \mathcal{F}_\eta \approx 0.1266, \ \mathcal{F}_\lambda \approx 0.1181, \ \mathcal{F}_\xi \approx 0.1645 \tag{23}$$

and equation (20) is satisfied by following similar arguments to those given in the proof of Proposition 1. □

4. Tilings for the compact Euclidean 3-manifolds

The fundamental polyhedra for the ten compact flat 3-manifolds are represented in Figs. 4 and 5. The front and back faces are glued as indicated by the letter *F*. The unmarked faces are glued straight across and the marked faces are glued as indicated by the small black and white rectangles. In Fig. 4, we can see two fundamental domains for the Hantzsche–Wendt space where the identifications are as shown by the letters *F*, *L*, *R*, *P*.

The tilings we want to consider have triangular prisms as prototiles (Fig. 10*a*). Depending on the axiom ω, the triangular faces grow by iterating the inflation rules defined by equations (3) or (7). The inflation rules for the rectangular faces are the Cartesian product of two one-dimensional substitutions. We

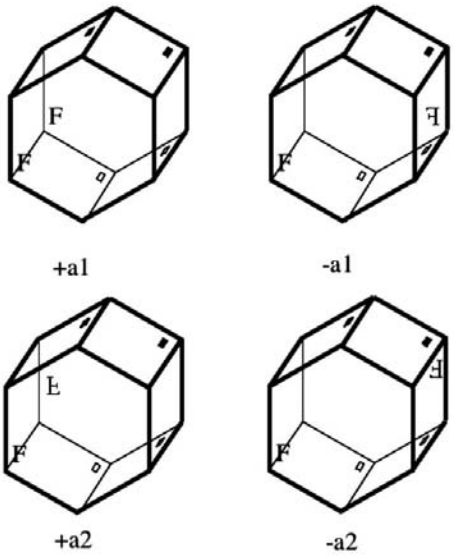

Figure 5
Fundamental domains for the non-orientable flat 3-manifolds.

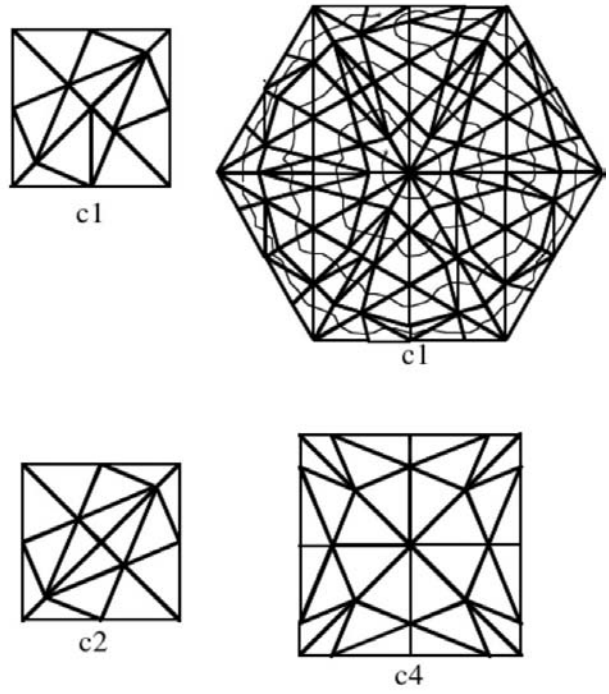

Figure 6
Pre-axioms for the faces marked with *F* of the fundamental polyhedra corresponding to *c*1, *c*2, *c*4. In the hexagonal face of the *c*1 polyhedron, we draw a path which allows us to describe the pre-axiom by a word without brackets [equation (25)].

choose the substitutions corresponding to the edges which are given by equations (4) and (8). In Fig. 10(*b*), we see an example for $d = 8$. The rectangular face has edges C, D and the first inflation step shown corresponds to the substitution rules given by equation (4). The axioms for the polygonal faces marked with letters in the fundamental polyhedra are $\omega = \Phi_d[\Xi]$, where Ξ denotes the pre-axiom. Only for some cases do we give the complete word. For the remaining cases, due to the words' length, we give only the first and the last letters of the words representing the pre-axioms. The complete words can be obtained by following the paths shown in Figs. 6–9. The patterns corresponding to ω are placed on the faces marked with the letter F in Figs. 4–5 and on the top and bottom faces for the Hantzsche–Wendt manifold. The pre-axioms, represented in Figs. 6–9, are the following ones.

(i) 3-Torus (*c*1)

(*a*) cubic 3-torus:

$$\Xi = e_{12}\widetilde{e}_2 e_4 d_{12} b_{15} b_1 d_{10} a_1 \widetilde{a}_{13} d_4 b_7 b_9 a_5 b_{13} a_9 \widetilde{a}_5; \qquad (24)$$

(*b*) hexagonal 3-torus:

$$\Xi = \theta_{10}\widetilde{\theta}_{22}\theta_{14} \ldots \widetilde{\mu}_{10}\widetilde{\theta}_{14}\lambda_{18}\widetilde{\theta}_6\theta_{22}\lambda_0\theta_{14}. \qquad (25)$$

(ii) Half-turn space (*c*2):

$$\Xi = \widetilde{e}_{10} e_{12}\widetilde{e}_2 e_4 d_{12} b_{15} b_1 d_{10} a_1 \widetilde{a}_{13} d_4 b_7 b_9 d_2 a_9 \widetilde{a}_5. \qquad (26)$$

(iii) Third-turn space (*c*3):

$$\Xi = \widetilde{\theta}_6\theta_{22}\widetilde{\theta}_{10} \ldots \lambda_8\widetilde{\mu}_6\mu_{10}\lambda_{22}\widetilde{\theta}_{18}. \qquad (27)$$

(iv) Quarter-turn space (*c*4):

$$\Xi = (\Phi_8[d_1])(\Phi_8[d_5])(\Phi_8[d_9])(\Phi_8[d_{13}]). \qquad (28)$$

(v) Sixth-turn space (*c*6):

$$\Xi = \widetilde{\theta}_{14}\theta_2\widetilde{\theta}_{10} \ldots \theta_{10}\widetilde{\theta}_{23}\widetilde{\mu}_{11}\mu_{13}. \qquad (29)$$

(vi) Hantzsche–Wendt space (*c*22):

$$\Xi = \widetilde{a}_{14}\widetilde{e}_{13}\widetilde{a}_4 b_6 \ldots e_{13}\widetilde{e}_5\widetilde{a}_6 d_1. \qquad (30)$$

(vii) Klein space ($+a1$):

$$\Xi = \lambda_{16}\theta_6\nu_{18}\widetilde{\nu}_{14}\widetilde{\theta}_2 \ldots \widetilde{\theta}_{18}\theta_6\widetilde{\theta}_{14}. \qquad (31)$$

(viii) Klein space with horizontal flip ($-a1$):

$$\Xi = \delta_6\gamma_5\beta_{16}\widetilde{\beta}_4\gamma_{15} \ldots \widetilde{\nu}_0\lambda_2\zeta_{15}\gamma_2\widetilde{\gamma}_{22}. \qquad (32)$$

(ix) Klein space with vertical flip ($+a2$):

$$\Xi = \theta_8\widetilde{\theta}_{20}\theta_{12} \ldots \widetilde{\epsilon}_0\lambda_2\theta_{16}\widetilde{\theta}_4\theta_{20}\widetilde{\theta}_8\lambda_{12}. \qquad (33)$$

(x) Klein space with half turn ($-a2$):

$$\Xi = \lambda_4\widetilde{\nu}_{11}\widetilde{\epsilon}_2\widetilde{\delta}_{13}\gamma_1 \ldots \eta_{17}\zeta_5\widetilde{\epsilon}_{18}\epsilon_6. \qquad (34)$$

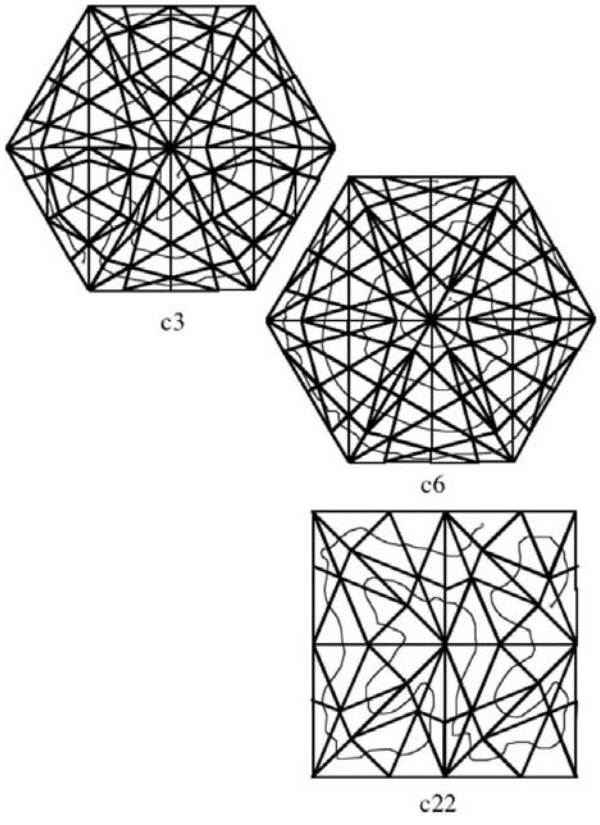

Figure 7
Pre-axioms for *c*3, *c*6, *c*22. The words in equations (27), (29) and (30) can be completed by following the paths indicated.

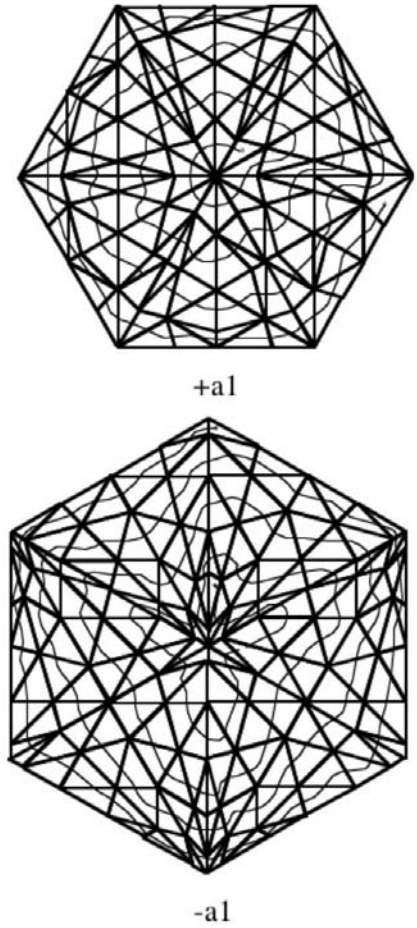

Figure 8
Pre-axioms for $+a1$, $-a1$ and paths for equations (31) and (32).

No brackets are necessary for the pre-axiom descriptions, but for simplicity we have used them in equation (28). Once we have the pattern in accordance with an axiom in the two parallel faces marked with letters in Figs. 4–5, we join up all the corresponding vertices by straight segments L parallel to the unmarked faces. This is the first tiling by triangular prisms. Then in the first inflation step applied to L (edge D in Fig. 10*b*), each vertex in the resulting one-dimensional tiling defines in a unique way a plane parallel to the marked faces. We place by parallel transport in each of this planes the triangle patterns of the marked faces and we join up again the corresponding vertices by straight segments. This procedure is repeated at each inflation step. By construction of the pre-axioms and because the words representing the inflated edges are palindromes [see equation (11)], the tilings for the ten compact Euclidean manifolds satisfy the face-to-face condition. Also, this condition is fulfilled by the three-dimensional random tilings induced by the non-deterministic substitution rules derived from equations (12) and (13), which determine also their configurational entropies. The reason is that the entropy computations performed in the proofs of Propositions 1 and 2 give results independent of the initial conditions about the tiles' content. If no additional entropic term is introduced in the three-dimensional constructions, then the entropies depend only on the type of inflation rules applied to the planar pre-axioms and not on their tile contents, and hence they are the same as in two dimensions.

In order to generate simplicial tilings, arrows can be placed on the edges with certain orientations. A triangular prism is decomposed into three tetrahedra in accordance with the arrow orientations as in Fig. 11(*a*). In addition to the cases studied in this work, other types of inflation factors and substitution rules are possible for some manifolds (Escudero, 2006*a*,*b*, 2007). In those cases, all the triangle edges have an arrow except the longest edge. There are two possibilities for each arrowed triangle. Either two of its edges are arrowed and the third is not or the three edges are arrowed. In the first case, the triangular prism can be decomposed into six tetrahedra as in Fig. 11(*b*), and in the second case into three. In some cases, we can also divide the rectangular face corresponding to an arrowed edge into four parts as in Fig. 11(*b*) and hence obtain a different structure. Although these simplicial decompositions are simpler, for the tilings studied in this work we choose a different one which does not introduce an additional entropic term and also generates face-to-face structures (Fig. 11*c*).

Step 1: We choose a point in the interior of the prism and we join up all the vertices with it by means of a straight line. In this way, we obtain two tetrahedra and three pyramids.

Step 2: Each pyramid is decomposed into four tetrahedra corresponding to the four triangles formed from the diagonal subdivision of their rectangular bases.

We can summarize the results already obtained in the following.

Theorem 1. The ten compact Euclidean 3-manifolds admit non-periodic tilings with triangular prisms as prototiles derived from recursive subdivisions of the faces with the following properties.

1. The rectangular faces are subdivided according to the Cartesian product of two one-dimensional substitutions.

2. The triangular faces are subdivided according to the inflation rules defined by equations (3) or (7) depending on the pre-axioms which are given by equations (24)–(34) and Figs. 6–9.

3. The tilings and their simplicial decompositions satisfy the face-to-face condition.

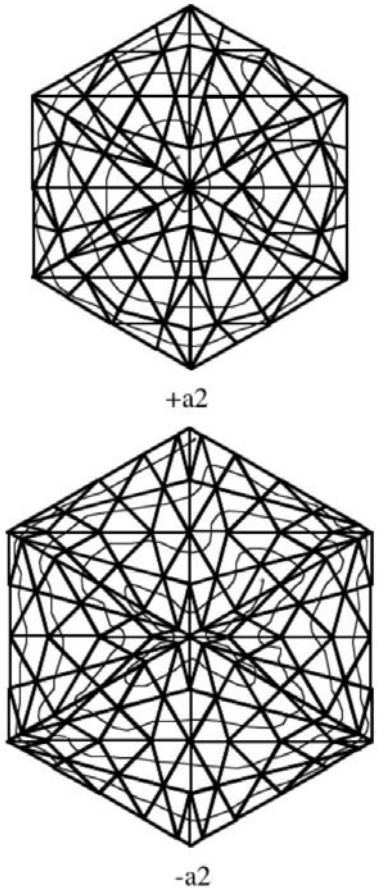

Figure 9
Pre-axioms for $+a2$, $-a2$ and paths for equations (33) and (34).

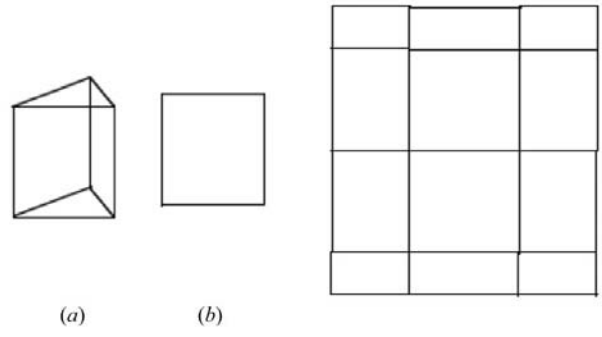

Figure 10
(*a*) The prototiles. (*b*) Inflation of a rectangular face for $d = 8$ with edges C (parallel to the x axis) and D (parallel to the y axis) and edge substitution rules given by equation (4).

4. The two-dimensional random tilings defined by equations (12) and (13) induce three-dimensional random tilings on the manifolds and the configurational entropies depend only on the information in the faces of the fundamental polyhedra.

5. Concluding remarks

Multiconnected manifolds have found applications in several fields. Motivated by the discovery of fullerene molecules and related forms of carbon, several authors have studied fullerenes on the torus and the Klein bottle (see Kirby & Pisanski, 1998, and references therein; Deza *et al.*, 2000). By defining a fullerene as a finite trivalent map with only five- and six-gonal faces embedded in a surface, the Euler characteristic formula permits the existence of only polyhexes for the torus and the Klein bottle. Also, extensions to space fullerenes as four-valent tilings of R^3 have been considered. The existence of aperiodic order in fullerenes has been studied by Fleming *et al.* (1991) and Michaud *et al.* (1998) although it is still not clear whether or not the growth is from nuclei with non-crystallographic symmetries.

A different context where multiconnected manifolds appear is in the study of the topology of the universe (Lachieze-Rey & Luminet, 1995; Levin, 2002; Luminet *et al.*, 2003; Kramer, 2005). A non-orientable 3-manifold was considered by Roukema & Edge (1997) in relation to the existence of ghost images of astrophysical objects. Linde has recently argued (Linde, 2004) that compact flat spatial sections should be considered typical in inflationary cosmologies and McInnes (2005) comes to the conclusion that only three of the ten compact manifolds are candidates for the explanation of the topology of the universe. On the other hand, in quantum gravity, different approaches to an underlying discrete space–time are Regge calculus, dynamical triangulations, graph-based theories such as loop quantum gravity, spin foam models or causal sets (Rovelli, 2004). Because the structures studied in this paper are based on a recursive procedure, they could be taken into account as a means to connect cosmic topology with simplicial quantum gravity theories. Although we have used two basic planar patterns, other types of higher planar symmetries (Escudero, 2006*b*) can be considered. There is strong evidence that the area of a surface limits the information content: black-hole entropy is proportional to the area of its surface and this is the highest entropy that a space–time region may have (Bousso, 2002). In our simplicial structures, the entropy is due to tile rearrangements in the faces of the fundamental polyhedra and the configurational entropy is consistent with the Bekenstein–Hawking bound.

In the tilings considered in this work, there are several possible alternatives for the choice of the edges perpendicular to the faces where the pre-axioms are defined. This fact can be useful in order to construct physical models, because one has to take into account that there is a freedom in the choice of the third dimension: oblate and prolate spaces give different contributions to the quadrupole (Riazuelo *et al.*, 2004). Some open questions that can also be of interest are the study of the existence of substitution rules for the prototiles obtained after the simplicial decompositions, the relationship with projection methods and iterative constructions of rhombus tilings and the analysis of the spectrum of the discrete Laplace operator.

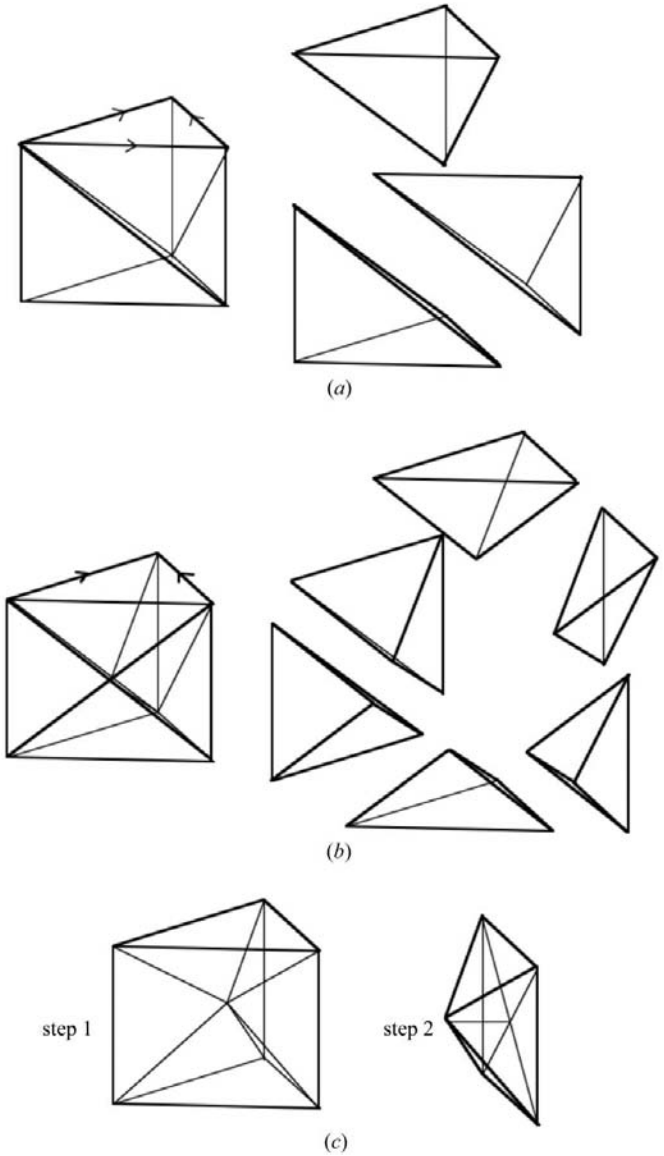

Figure 11
Simplicial decompositions: (*a*) three prototiles, (*b*) six prototiles, (*c*) fourteen prototiles.

References

Bousso, R. (2002). *Rev. Mod. Phys.* **74**, 825–874, http://arXiv.org/abs/hep-th/0203101v2.
Bruijn, N. G. de (1981). *Ned. Akad. Wetensch. Proc.* A**84**, 38–66.
Bruijn, N. G. de (1986). *J. Phys. Fr.* **47**, C**3-9**, 85–94.
Conway, J. H. & Rossetti, J. P. (2003). *Describing the platycosms*, http://arXiv.org/abs/Math.DG/0311476.

Destainville, N., Widom, M., Mosseri, R. & Bailly, F. (2005). *J. Stat. Phys.* **120**, 799–835.
Deza, M., Fowler, P. W., Rassat, A. & Rogers, K. M. (2000). *J. Chem. Inf. Comput. Sci.* **40**, 550–558.
Elser, V. (1985). *Phys. Rev. Lett.* **54**, 1730.
Escudero, J. G. (2000). *Mater. Sci. Eng.* A**294-296**, 389–392.
Escudero, J. G. (2001). *Int. J. Mod. Phys.* B**15**, 1165–1175.
Escudero, J. G. (2003). *Int. J. Mod. Phys.* B**17**, 2789–2790.
Escudero, J. G. (2004). *Int. J. Mod. Phys.* B**18**, 1595–1602.
Escudero, J. G. (2006*a*). *Philos. Mag.* **86**, 901–908.
Escudero, J. G. (2006*b*). International Congress of Mathematicians (ICM-2006), Madrid, Spain.
Escudero, J. G. (2007). *Philos. Mag.* **87**, 985.
Escudero, J. G. & Garcia, J. G. (2005). *J. Phys. A: Math. Gen.* **38**, 6525–6543.
Fleming, R. M., Kortan, A. R., Hessen, B., Siegriest, T., Thiel, F. A., Marsh, P., Haddon, R. C., Tycko, R., Dabbagh, G., Kaplan, M. L. & Mujsce, A. M. (1991). *Phys. Rev. B*, **44**, 888–891.
Hantschze, W. & Wendt, H. (1935). *Math. Ann.* **110**, 593–611.
Kenyon, R. (2000). *Directions in Mathematical Quasicrystals*, edited by M. Baake & R. V. Moody, pp. 307–328. CRM Monograph Series. Providence, RI: AMS.
Kenyon, R., Okounkov, A. & Sheffield, S. (2006). *Ann. Math.* **163**, 1019–1056.
Kirby, E. C. & Pisanski, T. (1998). *J. Math. Chem.* **23**, 151–167.
Kramer, P. (2005). *J. Phys. A: Math. Gen.* **38**, 3517–3540.
Lachieze-Rey, M. & Luminet, J. P. (1995). *Phys. Rep.* **254**, 135–214.
Levin, J. (2002). *Phys. Rep.* **365**, 251–333.
Linde, A. (2004). *J. Cosmol. Astropart*. **10**, 2–14. http://arxiv.org/abs/hep-th/0408164.
Luminet, J. P., Weeks, J., Riazuelo, A., Lehoucq, R. & Uzan, J. P. (2003). *Nature (London)*, **425**, 593–595.
McInnes, B. (2005). *Nucl. Phys.* B**709**, 213–240, http://arxiv.org/abs/hep-th/0410115.
Michaud, F., Barrio, M., Toscani, S., Lopez, D. O., Tamarit, J. Ll., Agafonov, V., Szwarc, H. & Ceolin, R. (1998). *Phys. Rev. B*, **57**, 10351–10358.
Nischke, K. P. & Danzer, L. (1996). *Discrete Comput. Geom.* **15**, 221–236.
Nowacki, W. (1934). *Comment. Math. Helv.* **7**, 81–93.
Randall, D. & Yngve, G. (2000). 11th SIAM/ACM Symposium on Discrete Algorithms (SODA), pp. 1–10.
Riazuelo, A., Weeks, J. R., Uzan, J. P., Lehoucq, R. & Luminet, J. P. (2004) *Phys. Rev. D*, **69**, 103518.
Rossetti, J. P. & Conway, J. H. (2006). *Math. Res. Lett.* **13**, 475–494.
Roukema, B. F. & Edge, A. C. (1997). *Mon. Not. R. Astron. Soc.* **292**, 105–112.
Rovelli, C. (2004). *Quantum Gravity*. Cambridge University Press.
Shaw, L. J., Elser, V. & Henley, C. L. (1991). *Phys. Rev. B*, **43**, 3423–3433.
Strandburg, K. J. (1991). *Phys. Rev. B*, **44**, 4644–4646.
Thurston, W. P. (1997). *Three-Dimensional Geometry and Topology*. Princeton University Press.
Widom, M., Mosseri, R., Destainville, N. & Bailly, F. (2002). *J. Stat. Phys.* **109**, 945–965.
Wolfram, S. (1991). *Mathematica*. New York: Addison–Wesley Publishing.